

SCIENTIFIC REPORTS

OPEN

SDS-induced oligomerization of Lys49-phospholipase A₂ from snake venom

Takashi Matsui¹, Shizuka Kamata¹, Kentaro Ishii², Takahiro Maruno³, Nouran Ghanem¹, Susumu Uchiyama^{2,3}, Koichi Kato^{2,4,5}, Atsuo Suzuki⁶, Naoko Oda-Ueda⁷, Tomohisa Ogawa¹ & Yoshikazu Tanaka^{1,8}

Phospholipase A₂ (PLA₂) is one of the representative toxic components of snake venom. PLA₂s are categorized into several subgroups according to the amino acid at position 49, which comprises either Asp49, Lys49, Arg49 or Ser49. Previous studies suggested that the Lys49-PLA₂ assembles into an extremely stable dimer. Although the behavior on Sodium dodecyl sulfate-polyacrylamide gel electrophoresis (SDS-PAGE) under reducing or non-reducing conditions suggested the presence of intermolecular disulfide bonds, these bonds were not observed in the crystal structure of Lys49-PLA₂. The reason for this discrepancy between the crystal structure and SDS-PAGE of Lys49-PLA₂ remains unknown. In this study, we analyzed a Lys49-PLA₂ homologue from *Protobothrops flavoviridis* (PflLys49-PLA₂ BP1I), by biophysical analyses including X-ray crystallography, SDS-PAGE, native-mass spectrometry, and analytical ultracentrifugation. The results demonstrated that PflLys49-PLA₂ BP1I spontaneously oligomerized in the presence of SDS, which is one of the strongest protein denaturants.

Snakebite induces acute myonecrosis as well as other biological effects including hemolytic, neurotoxic, cardiotoxic, anticoagulant and antiplatelet activities of multiple complex protein assemblies. These protein complexes are composed of various multi-locus gene families that underwent accelerated evolution¹. Phospholipase A₂ (PLA₂, EC 3.1.1.4) is one of the representative toxic components of snake venom. Snake venom PLA₂s are classified into groups I and II based on disulfide bond patterns. Group II PLA₂s are further categorized into several subgroups based on the amino acid at position 49. These subgroups contain Asp49, Lys49, Arg49 or Ser49, among which Asp49 and Lys49 are the most common. Although PLA₂s share high sequence similarity, their phospholipase activity is distinct. Asp49-PLA₂ hydrolyzes the *sn*-2 ester bond of the membrane phospholipids to generate fatty acids and lysophospholipids in a Ca²⁺ dependent manner. The Asp49 coordinating on the Ca²⁺ ion acts as a catalytic residue for hydrolysis of the ester bond^{2,3}. In contrast, Lys49-PLA₂ lacks phospholipase activity, or exhibits minimal phospholipase activity because the catalytic Asp49 is substituted for Lys⁴⁻⁶. Despite the absence of phospholipase activity, Lys49-PLA₂ exhibits myonecrotic activity due to the intrinsic function of its C-terminal region that is abundant in positive and hydrophobic residues⁷⁻⁹ which mediate caspase-independent apoptosis¹⁰.

Previous studies showed that the Lys49-PLA₂ forms an extremely stable dimer which is not dissociated to monomers even in the presence of 0.1% (w/v) sodium dodecyl sulfate (SDS) and 2 M urea¹¹. Even though each monomer shares a similar structure¹², X-ray crystallography studies^{4,5,7,9,13-22} revealed two distinct dimer types: the conventional dimer and the alternative dimer. These dimers differ in their myotoxicity activity: the conventional dimer comprises the inactive state and the alternative dimer comprises the active form¹². In the

¹Graduate School of Life Sciences, Tohoku University, 2-1-1 Katahira, Aoba-ku, Sendai, Miyagi, 980-8577, Japan.

²Exploratory Research Center on Life and Living Systems (EXCELLS), National Institutes of Natural Sciences, 5-1 Higashiyama, Myodaiji-cho, Okazaki, 444-8787, Japan. ³Graduate School of Engineering, Osaka University, 2-1 Yamadaoka, Suita, Osaka, 565-0871, Japan. ⁴Graduate School of Pharmaceutical Sciences, Nagoya City University, 3-1 Tanabe-dori, Mizuho-ku, Nagoya, 467-8603, Japan. ⁵Institute for Molecular Science, National Institutes of Natural Sciences, 5-1 Higashiyama, Myodaiji-cho, Okazaki, 444-8787, Japan. ⁶Department of Biomolecular Engineering, Graduate School of Engineering, Nagoya University, Furo-cho, Chikusa-ku, Nagoya, 464-8603, Japan.

⁷Faculty of Pharmaceutical Sciences, Sojo University, 4-22-1 Ikeda, Nishi-ku, Kumamoto, 860-0082, Japan. ⁸Japan Science and Technology Agency, PRESTO, 2-1-1 Katahira, Aoba-ku, Sendai, 980-8577, Japan. Takashi Matsui and Shizuka Kamata contributed equally. Correspondence and requests for materials should be addressed to Y.T. (email: yoshikazu.tanaka@tohoku.ac.jp)

conventional dimer, two protomers interact via their β -wings and N-terminal α -helices. Compared with the conventional dimer, the alternative dimer contains a larger contact surface, generating a compact dimer conformation. The alternative dimer formation was also supported by the results of small angle X-ray scattering (SAXS)^{21,23}. The gyration radius (R_g) calculated from SAXS showed good agreement with the alternative dimer rather than the conventional dimer, suggesting that the alternative dimer has a more stable conformation in solution²¹.

Previous studies have shown that when Lys49-PLA₂ is subjected to non-reducing SDS-polyacrylamide gel electrophoresis (PAGE), a band is generated at the position corresponding to the oligomer, and the band shifts to the position of monomer in the presence of dithiothreitol¹¹. These observations suggest that Lys49-PLA₂ contains intermolecular disulfide bonds. However, intermolecular disulfide bonds were not observed in any solved crystal structure of Lys49-PLA₂. The reason for this discrepancy between the crystal structure and SDS-PAGE of Lys49-PLA₂ remains unknown. Clarification of these inconsistent results may provide insight into the physiological function of this protein.

In this study, we comprehensively analyzed basic protein II (BP II), which is one of the Lys49-PLA₂ homologues isolated from the venom of *Protobothrops flavoviridis* (PflLys49-PLA₂ BP II)^{6,24,25}. Our biophysical analyses included X-ray crystallography, SDS-PAGE, native-mass spectrometry (Native-MS), and analytical ultracentrifugation. The results demonstrated that PflLys49-PLA₂ BP II spontaneously oligomerized in the presence of SDS.

Materials and Methods

Purification of PflLys49-PLA₂ BP II. *P. flavoviridis* was collected at Amami Oshima Island, Kagoshima prefecture in Japan in accordance with Japanese guidelines and regulations under the law of humane treatment and management of animals as a dangerous animal. Collecting venoms was conducted after carbonic anesthesia or giving an electric shock for habu snake according to the experimental plan authorized by the Institute of Medical Science, the University of Tokyo. By this method, the pain of habu can be alleviated and accidental bite can be prevented. Snake venom was extracted from *P. flavoviridis* and was frozen quickly under liquid nitrogen and then lyophilized. The lyophilized venom was dissolved in Milli-Q water and was loaded onto a CM52 cation exchange column (15 mm i.d. x 870 mm) pre-equilibrated with 20 mM ammonium acetate buffer pH 6.8 containing 0.1 mM CaCl₂. The bound PflLys49-PLA₂ BP II (UniProt ID: P0DJJ9)^{6,24,25} was eluted with a linear gradient of 20–500 mM ammonium acetate. The fractions containing PflLys49-PLA₂ BP II were collected and dialyzed against Milli-Q water three times utilizing a cellulose membrane (MWCO 10 kDa). The dialyzed sample was subsequently lyophilized, and stored until use.

Sodium dodecyl sulfate-polyacrylamide gel electrophoresis (SDS-PAGE) analysis. The purity and electrophoretic characteristics of PflLys49-PLA₂ BP II were analyzed by 15% (w/v) SDS-PAGE followed by Coomassie Blue staining. In order to confirm the presence of intermolecular disulfide bonds, the object protein was mixed with SDS-PAGE sample buffer [62.5 mM Tris-HCl pH 6.8, 2% (w/v) SDS and 5% (w/v) sucrose] with or without 5% (v/v) 2-mercaptoethanol (2-ME). To assess the conformation of the oligomerization states in the crystal, the protein crystals were picked up from the drop, and washed three times with crystallization buffer. Next, the crystals were dissolved in SDS-PAGE sample buffer without 2-ME. All samples were incubated at 95 °C for 5 min and loaded onto the SDS-PAGE gel.

Crystallization and X-ray crystallography. The concentration of the lyophilized protein was adjusted to 20 mg/ml with Milli-Q water. All crystallization attempts were performed using the sitting-drop vapor diffusion technique at 20 °C. Diffraction-quality crystals of the object protein were obtained with the optimized reservoir conditions [100 mM sodium acetate pH 4.2, 500 mM ammonium acetate, and 32.5% (w/v) PEG4000] after initial screenings using 96-condition crystallization screening kits (Qiagen, Hilden, Germany). All crystallization drops were prepared by mixing 1.0 μ l of PflLys49-PLA₂ BP II with an equal volume of reservoir solution followed by equilibration of the mixtures against 50 μ l of reservoir solution. The PflLys49-PLA₂ BP II crystals were added to a crystallization solution containing 20% (v/v) ethylene glycol as a cryoprotectant. After a few seconds, the crystals were picked up in a nylon loop and then flash-cooled to 100 K in a nitrogen gas stream. The X-ray diffraction experiments were performed at the Photon Factory (proposals 16G092 and 17G595) and SPring-8 (proposals 2015B6524, 2016A2565 and 2016B2565). X-ray diffraction data sets were collected on the BL-17A beamline at the Photon Factory (Tsukuba, Japan). The diffraction data of the crystals were processed and scaled with XDS²⁶. The molecular replacements were performed with BspSP-7 (PDB code 5VFH)¹⁶ as the search model using Phaser²⁷. The structure refinement of PflLys49-PLA₂ BP II was performed using phenix.refine²⁸, with the twin operators of (h, -h-k, -l) with a fraction of 0.49. The structure was modified manually with COOT²⁹. The quality of the final models was assessed with MolProbity³⁰. All crystallographic figures were prepared with PyMOL³¹. The crystallographic data and refinement statistics are summarized in Table 1. The coordinate and structure factor data of PflLys49-PLA₂ BP II reported in this paper have been deposited under the accession number 6AL3.

Native-MS analysis. Native-MS analysis was performed as described previously³². Briefly, 50 μ M of BP II aqueous solution was measured by nanoflow electrospray ionization mass spectrometry using gold-coated glass capillaries made in house with approximately 2–5 μ L of sample loaded per analysis. The spectra were recorded on a SYNAPT G2-Si HDMS mass spectrometer (Waters, Milford, Massachusetts, USA) in positive ionization mode at 1.33 kV with a 150 V sampling cone voltage and source offset voltage, 0 V trap and transfer collision energy, and 5 mL/min trap gas flow. The spectra were calibrated using 1 mg/mL cesium iodide and analyzed using MassLynx software (Waters).

Sedimentation velocity analytical ultracentrifugation (SV-AUC). SV-AUC experiments were conducted with 1 mg/mL of PflLys49-PLA₂ BP II in the presence or absence of 1% (w/v) SDS. Data collection was performed at 20 °C in a ProteomeLab XL-I analytical ultracentrifuge (Beckman Coulter, Brea, California,

Sample name	Lys49-PLA ₂ BPII
PDB entry	6AL3
Data collection	
Beamline	PF BL-17A
Wavelength (Å)	0.98000
Space group	<i>P</i> 6 ₄
Unit cell parameters	
a, b, c (Å)	126.9, 126.9, 64.9
α, β, γ (°)	90, 90, 120
Resolution range (Å)	50.0–2.57 (2.72–2.57)
Completeness (%)	99.9 (99.8)
<I/σ(I)>	12.6 (3.0)
R _{merge} (%)	12.3 (56.4)
CC/2	100.0 (84.6)
Multiplicity	6.7 (6.9)
No. of observed reflections	129,632 (21,169)
No. of unique reflections	19,245 (3,080)
Refinement	
Resolution (Å)	45.4–2.57
R _{work} (%)	21.8
R _{free} (%)	24.5
Twin fraction (%)	0.49 (<i>h</i> , <i>-h-k</i> , <i>-l</i>)
r.m.s.d. from ideal	
bond length (Å)	0.006
bond angle (°)	0.954
No. of molecules per asymmetric unit	4
Ramachandran plot	
favoured region	91.9
allowed region	7.9
outlier region	0.2
Total atoms	3,835
Average B-factor (Å ²)	43.0

Table 1. Data collection and refinement statistics.

USA) at 60,000 rpm using UV detection. The collected data were analyzed using the continuous *c*(*s*) distribution from the program SEDFIT (version 15.01b)³³ with fitting for the frictional ratio, meniscus, and time-invariant noise with a regularization level of 0.68. The partial specific volume of *Pfl*Lys49-PLA₂ BPII was calculated as 0.728 cm³ g⁻¹ using the program SEDNTERP 1.09. The buffer density and viscosity of each condition were determined using a DMA 5000 densitometer (Anton Paar, Graz, Austria) and a Lovis 2000M viscometer (Anton Paar), respectively. The resulting data were analyzed with the program SEDNTERP 1.09. The partial specific volume of *Pfl*Lys49-PLA₂ BPII in the presence of 1% (w/v) SDS was determined experimentally by using density contrast SV-AUC^{34,35} where the samples with identical protein concentrations but different H₂O/D₂O ratios (H₂O 80%/D₂O 20% and H₂O 40%/D₂O 60%) were subjected to a sedimentation velocity run. The data were analyzed by setting the partial specific volume as a floated parameter in the “Hybrid Global Continuous Distribution and Global Discrete Species” model in the program SEDPHAT (version 12.1b)³⁶. The partial specific volume and molecular mass of the SDS micelle were assumed to be 0.870 cm³ g⁻¹ and 14,000 Da, respectively^{37,38}.

Results

Crystal structure of *Pfl*Lys49-PLA₂ BPII. The crystal structure of *Pfl*Lys49-PLA₂ BPII was determined at a resolution of 2.57 Å. The asymmetric unit contained four molecules of *Pfl*Lys49-PLA₂ BPII (Fig. 1a). These four molecules were superimposed well relative to each other with root-mean-square-deviation (r.m.s.d.) values less than 0.5 Å for the Cα-atoms (Fig. 1b). All 14 Cys residues formed the following seven intramolecular disulfide bonds (Fig. 1c): Cys26–Cys116, Cys28–Cys44, Cys43–Cys96, Cys49–Cys122, Cys50–Cys89, Cys57–Cys82, and Cys75–Cys87. Ca²⁺ ions, which are important for the phospholipase activity of other Lys49-PLA₂s was not bound on the catalytic site of *Pfl*Lys49-PLA₂ BPII due to the substitution of Asp49 for Lys^{4,5,7,13–15,17,20,22,39}.

The relative orientation between molecules A and B was similar to that between molecules C and D (Fig. 1d). The r.m.s.d. between molecules B and D after superimposing molecules A and C was 1.3 Å, which suggested the possibility that this dimer is an intrinsic dimer structure of *Pfl*Lys49-PLA₂ BPII. However, this dimer was superimposed neither on the conventional dimer nor the alternative dimer previously reported (Fig. 1e,f). Furthermore, basic residues were located on both sides of the interface, and the surface charges of both interfaces were positive (Fig. 1g). The area of the interface among four molecules was less than 350 Å². Based on these

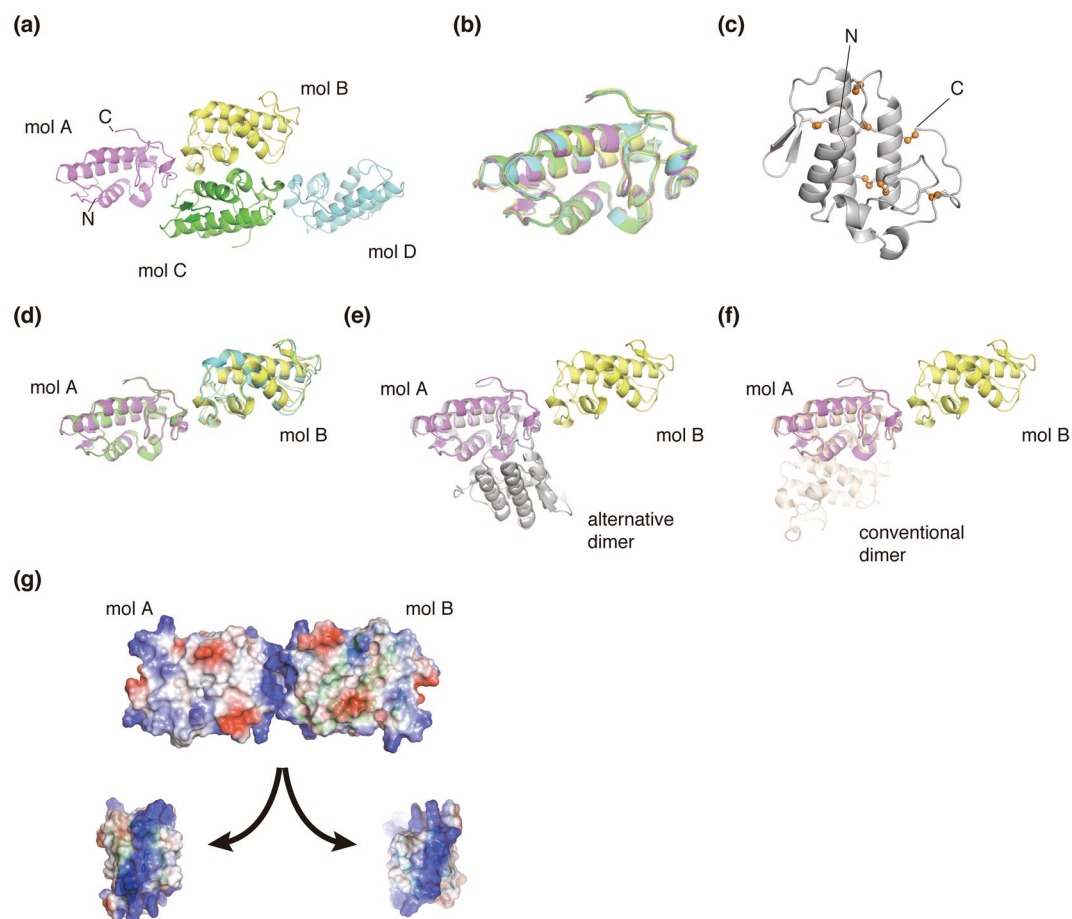


Figure 1. X-ray crystal structure of *PflLys49-PLA₂ BPII*. **(a)** Crystal structures of four molecules in an asymmetric unit. **(b)** Superimposition of the four molecules. **(c)** Disulfide bond network. The sulfur atoms are indicated as orange spheres. **(d)** Superimposition of molecules A and B on molecules C and D. **(e)** Superimposition of an alternative dimer (gray, PDB ID: 2Q2J) on molecule A of *PflLys49-PLA₂ BPII*. **(f)** Superimposition of the conventional dimer (wheat PDB ID: 2Q2J) on molecule A of *PflLys49-PLA₂ BPII*. **(g)** Surface charge distributions of the surface between molecules A and B. Surfaces comprising positive and negative charges are depicted as blue and red colors, respectively.

observations, we concluded that the conserved relative orientation between molecules is merely preferable packing in the crystal and *PflLys49-PLA₂ BPII* does not form any oligomers in the crystal.

The mobility of *PflLys49-PLA₂ BPII* in SDS-PAGE. The mobility of *PflLys49-PLA₂ BPII* was analyzed by SDS-PAGE (Fig. 2a). *PflLys49-PLA₂ BPII* without 2-ME treatment migrated at approximately 27 kDa when subjected to SDS-PAGE. On the other hand, *PflLys49-PLA₂ BPII* treated with 5% (v/v) 2-ME shifted to the position of approximately 14.4 kDa (Fig. 1a, lane 2). In general, the 2-ME-mediated band shift of *PflLys49-PLA₂ BPII* subjected to SDS-PAGE suggested the presence of intermolecular disulfide bond formation. However, all cysteine residues formed intramolecular disulfide bonds in the crystal structure (Fig. 1c), and thus, intermolecular disulfide bond formation is highly unlikely. These observations suggested that *PflLys49-PLA₂ BPII* may exhibit unusual behavior when subjected to SDS-PAGE. Therefore, we analyzed the mobility of *PflLys49-PLA₂ BPII* under a variety of conditions (Fig. 2b,c).

First, we evaluated the effect of urea, a typical protein denaturation reagent, on oligomerization. *PflLys49-PLA₂ BPII* was still oligomerized when subjected to SDS-PAGE in the presence of 6 M urea (Fig. 2b, lane 1). However, heat treatment in the presence of 6 M urea resulted in the dissociation of *PflLys49-PLA₂ BPII* to monomers (Fig. 2b, lane 2). It should be noted that a reducing reagent was not added to these samples. These results showed that the stable oligomer formation of *PflLys49-PLA₂ BPII* subjected to SDS-PAGE is not due to disulfide bond formation.

Next, we loaded crystals of *PflLys49-PLA₂ BPII* dissolved in the SDS-PAGE sample buffer containing 2% (w/v) SDS. Surprisingly, *PflLys49-PLA₂ BPII*, which adopted a monomeric form with no intermolecular disulfide bonds in the crystals, oligomerized after being subjected to SDS-PAGE (Fig. 2c). These observations suggested that treatment with the SDS-PAGE sample buffer induced oligomerization of this protein.

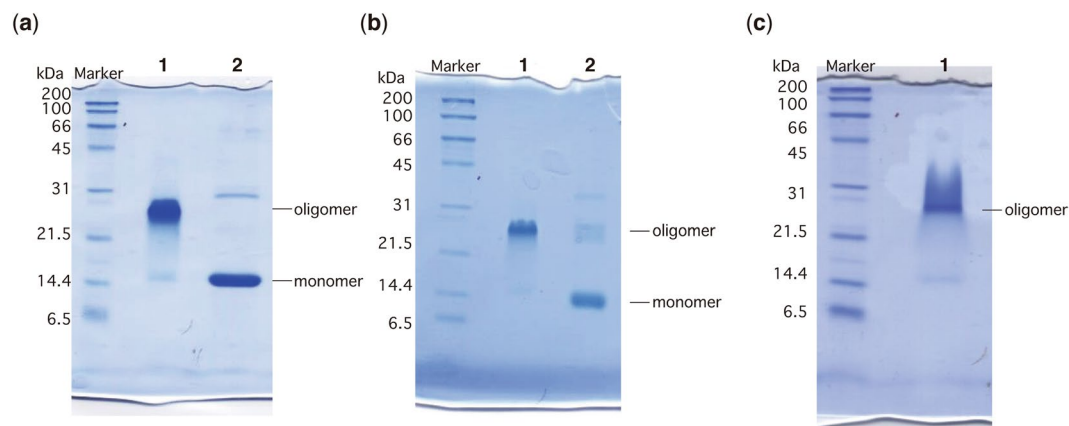


Figure 2. SDS-PAGE of *PflLys49-PLA₂* BPII under various conditions. (a) *PflLys49-PLA₂* BPII with and without 2-ME treatment. Lane 1, without 2-ME; lane 2, with 2-ME. (b) *PflLys49-PLA₂* BPII treated with 6 M urea. Lane 1, without 95 °C treatment; lane 2, after 95 °C treatment. (c) Resuspension of *PflLys49-PLA₂* BPII crystals with SDS-PAGE sample buffer.

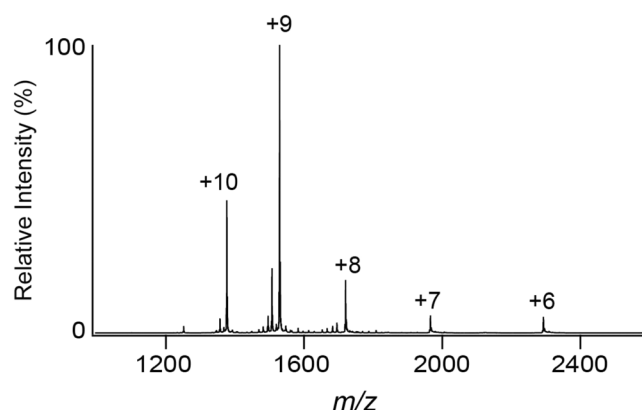


Figure 3. Native mass spectrum of *PflLys49-PLA₂* BPII. Native mass spectrum of 50 μ M *PflLys49-PLA₂* BPII dissolved in water was measured under the positive ionization mode.

Oligomerization state analyzed by native-MS and SV-AUC. To identify the oligomerization state of *PflLys49-PLA₂* BPII in an aqueous condition with neither detergent nor denaturant, the molecular mass distributions of 50 μ M of the purified *PflLys49-PLA₂* BPII dissolved in water were analyzed by native-MS. The molecular mass of *PflLys49-PLA₂* BPII in water was determined to be 13,753 Da, which is in good agreement with the estimated molecular mass of the deduced amino acid sequence (13,872 Da) (Fig. 3). It should be noted that native-MS analysis detected no oligomer. These results revealed that *PflLys49-PLA₂* BPII exists as a monomer in an aqueous solution.

Next, the effect of SDS on the oligomerization state of *PflLys49-PLA₂* BPII was analyzed by analytical ultracentrifugation. Purified *PflLys49-PLA₂* BPII dissolved in 20 mM Tris-HCl pH 8.0 and 200 mM NaCl at a concentration of 1 mg/mL distributed as a monomer with a molecular mass of 13.1 kDa (Fig. 4a, Table 2). This result is in good agreement with the native-MS observations described above (Fig. 3). In contrast to the monomeric state of *PflLys49-PLA₂* BPII dissolved in 20 mM Tris-HCl pH 8.0 and 200 mM NaCl, the sedimentation coefficients of *PflLys49-PLA₂* BPII in the presence of SDS exhibited a bimodal distribution. The sedimentation coefficients significantly increased compared to those obtained in the absence of SDS (Fig. 4b).

The density contrast SV-AUC analysis revealed that the partial specific volume of *PflLys49-PLA₂* BPII in the presence of SDS was $0.771 \text{ cm}^3 \text{ g}^{-1}$. Three possible protein-SDS complexes that have a partial specific volume of $0.771 \text{ cm}^3 \text{ g}^{-1}$ are as follows: (*PflLys49-PLA₂* BPII)(SDS)₂₁, (*PflLys49-PLA₂* BPII)₂(SDS)₄₂, and (*PflLys49-PLA₂* BPII)₃(SDS)₆₃ of which the calculated molecular masses were 19.9 kDa, 39.9 kDa, and 59.8 kDa, respectively (Fig. 4c,d). The molecular masses obtained from *c(s)* analysis of the two peaks (under the assumption that the three complexes have a similar molecular shape) were 33.1 kDa for the 2.6 S peak and 48.3 kDa for the 3.4 S peak (Fig. 4b, Table 2). These results lead to the conclusion that *PflLys49-PLA₂* BPII forms SDS bound dimers and SDS bound trimers in the presence of 1% (w/v) SDS.

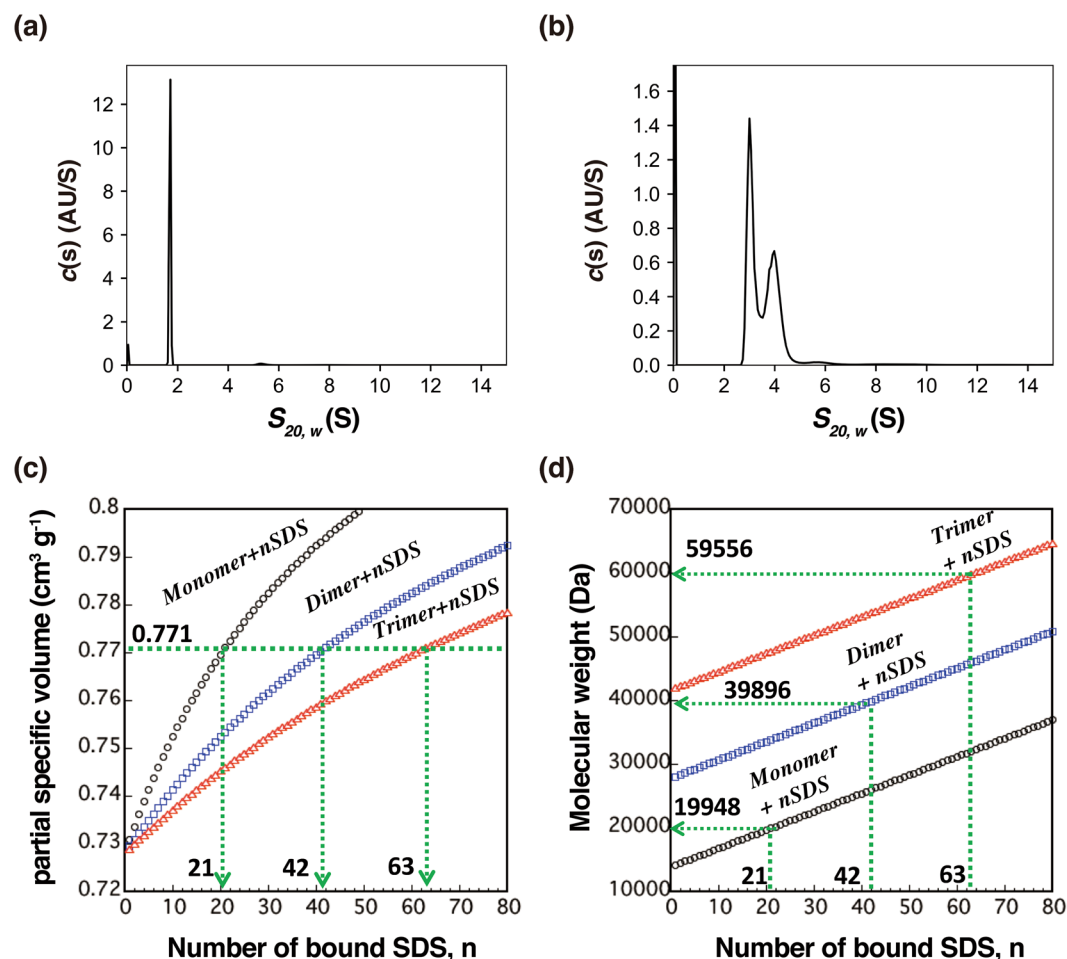


Figure 4. SV-AUC analysis of *PflLys49-PLA₂* BPII. Distribution of the sedimentation coefficients of *PflLys49-PLA₂* BPII in the absence (a) or presence (b) of 1% (w/v) SDS. The relationship between the number of bound SDS molecules and the partial specific volume (c) or molecular mass (d) of the complexes.

Condition	$s_{20,w}$	% of total	f/f_0	Estimated M_w (kDa)
Without SDS				
	1.7	95.6	1.18	13.1
	5.4	2.5		72.6
With SDS				
	2.6	53.9	1.24	33.1
	3.4	43.6		48.3

Table 2. $c(s)$ analysis of SV-AUC experiments in the presence or absence of 1% (w/v) SDS.

Discussion

Previous studies reported that Lys49-PLA₂s exist as either conventional or alternative dimers, based on the results of X-ray crystallography, electrophoresis, dynamic light scattering, and spectroscopy^{11,12,14,15,19,23,39–42}. In contrast to these previous reports, our present crystal structure showed that *PflLys49-PLA₂* BPII exists as a monomer in the crystal (Fig. 1). This was consistent with the results of native-MS (Fig. 3) and analytical ultracentrifugation analyses (Fig. 4), both of which showed that monomeric *PflLys49-PLA₂* BPII was detected in the absence of SDS. These results indicated that *PflLys49-PLA₂* BPII exists as a monomer in both solution and crystal states.

Although the behavior of *PflLys49-PLA₂* BPII in the crystal and solution states was distinct from Lys49-PLA₂s from other species (i.e., *PflLys49-PLA₂* BPII is a monomer while other Lys49-PLA₂s assemble to dimers), the behavior upon SDS-PAGE was similar between *PflLys49-PLA₂* BPII and other Lys49-PLA₂s. Specifically, both proteins oligomerized upon SDS-PAGE. The dissolved crystals of *PflLys49-PLA₂* BPII formed oligomers upon SDS-PAGE, which demonstrated that during sample preparation and/or electrophoresis the oligomerization of *PflLys49-PLA₂* BPII occurred spontaneously (Fig. 2c). Moreover, analytical ultracentrifugation indicated that 1% (w/v) SDS induces dimerization and trimerization of *PflLys49-PLA₂* BPII (Fig. 4). Taking these observations

together, we concluded that *PfLys49-PLA₂* BPII assembles to form SDS-resistant stable oligomers in the presence of 1% (w/v) SDS. Kilby and coworkers also reported a similar phenomenon, i.e., the interaction of SDS micelles with bovine PLA₂ induced trimer formation, in which approximately three molecules of bovine PLA₂ was predicted to bind one SDS micelle^{43,44}. The results of our analytical ultracentrifugation showed that *PfLys49-PLA₂* BPII assembles to form dimers and trimers. *PfLys49-PLA₂* BPII may assemble to form oligomers in a similar manner as bovine PLA₂. Notably, this characteristic of *PfLys49-PLA₂* BPII in SDS-PAGE did not change even in the presence of crude snake venom (Supplementary Fig. 1), indicating no significant synergy effect from another venom components to the behavior against SDS.

It is important to note that SDS, one of the strongest protein denaturants, induces oligomerization of *PfLys49-PLA₂* BPII. Thus, *PfLys49-PLA₂* BPII exhibits outstandingly strong stability against chemical denaturation. Indeed, oligomers of *PfLys49-PLA₂* BPII did not dissociate even in the presence of 6 M urea, and further heat treatment was necessary for the dissociation to monomers (Fig. 2). *PfLys49-PLA₂* BPII harbors seven intramolecular disulfide bonds, thus 12% of the total 122 amino acids (14 Cys residues) contributes to covalent bond formation. Such a large number of intramolecular disulfide bonds may contribute to this unusual behavior of this protein, i.e., oligomerization by a protein denaturant.

In the present study, we demonstrated that SDS induces oligomerization of *PfLys49-PLA₂* BPII. SDS can be regarded as a simple phospholipid analogue. These oligomers may also be induced by phospholipids, and the oligomer may interact with the membrane and function as a myotoxic agent to disrupt the cell membrane. Although the physiological significance of SDS-induced oligomerization of *PfLys49-PLA₂* BPII is still unclear, it may play a key role in its myotoxic function.

References

- Shibata, H. *et al.* The habu genome reveals accelerated evolution of venom protein genes. *Sci. Rep.* **8**, 11300 (2018).
- Verheij, H. M. *et al.* Methylation of Histidine-48 in Pancreatic Phospholipase A₂. Role of Histidine and Calcium Ion in the Catalytic Mechanism. *Biochemistry* **19**, 743–750 (1980).
- Scott, D. L. *et al.* Interfacial catalysis: The mechanism of phospholipase A₂. *Science* **250**, 1541–1546 (1990).
- Holland, D. R. *et al.* The Crystal Structure of a Lysine 49 Phospholipase A₂ from the Venom of the Cottonmouth Snake at 2.0 Å Resolution. *J. Biol. Chem.* **265**, 17649–17656 (1990).
- Fernandes, C. A. H. *et al.* Comparison between apo and complexed structures of bothropstoxin-I reveals the role of Lys122 and Ca²⁺-binding loop region for the catalytically inactive Lys49-PLA₂s. *J. Struct. Biol.* **171**, 31–43 (2010).
- Liu, S. Y. *et al.* Purification and amino acid sequence of basic protein II, a lysine-49-phospholipase A₂ with low activity, from *Trimeresurus flavoviridis* venom. *J. Biochem.* **107**, 400–408 (1990).
- Arni, R. K., Ward, R. J., Gutierrez, J. M. & Tulinsky, A. Structure of a calcium-independent phospholipase-like myotoxic protein from *Bothrops asper* venom. *Acta Crystallogr. - Sect. D Biol. Crystallogr.* **51**, 311–317 (1995).
- Chioato, L. *et al.* Mapping of the structural determinants of artificial and biological membrane damaging activities of a Lys49 phospholipase A₂ by scanning alanine mutagenesis. *Biochim. Biophys. Acta - Biomembr.* **1768**, 1247–1257 (2007).
- Murakami, M. T. *et al.* Inhibition of myotoxic activity of *Bothrops asper* myotoxin II by the anti-trypanosomal drug suramin. *J. Mol. Biol.* **350**, 416–426 (2005).
- Murakami, T. *et al.* A [Lys⁴⁹]-phospholipase A₂ from *Protobothrops flavoviridis* Venom Induces Caspase-Independent Apoptotic Cell Death Accompanied by Rapid Plasma-Membrane Rupture in Human Leukemia Cells. *Biosci. Biotechnol. Biochem.* **75**, 864–870 (2011).
- Francis, B., Gutierrez, J. M., Lomonte, B. & Kaiser, I. I. Myotoxin II from *Bothrops asper* (terciopelo) venom is a lysine-49 phospholipase A₂. *Arch. Biochem. Biophys.* **284**, 352–359 (1991).
- Fernandes, C. A. H., Borges, R. J., Lomonte, B. & Fontes, M. R. M. A structure-based proposal for a comprehensive myotoxic mechanism of phospholipase A₂-like proteins from viperid snake venoms. *Biochim. Biophys. Acta - Proteins Proteomics* **1844**, 2265–2276 (2014).
- Fernandes, C. A. H. *et al.* Structural bases for a complete myotoxic mechanism: Crystal structures of two non-catalytic phospholipases A₂-like from *Bothrops brazili* venom. *Biochim. Biophys. Acta - Proteins Proteomics* **1834**, 2772–2781 (2013).
- Ambrosio, A. L. B. *et al.* A molecular mechanism for Lys49-phospholipase A₂ activity based on ligand-induced conformational change. *J. Biol. Chem.* **280**, 7326–7335 (2005).
- Murakami, M. T., Melo, C. C., Angulo, Y., Lomonte, B. & Arni, R. K. Structure of myotoxin II, a catalytically inactive Lys⁴⁹-phospholipase A₂ homologue from *Atropoides nummifer* venom. *Acta Crystallogr. Sect. F Struct. Biol. Cryst. Commun.* **62**, 423–426 (2006).
- de Lima, L. F. G., Borges, R. J., Viviescas, M. A., Fernandes, C. A. H. & Fontes, M. R. M. Structural studies with BnSP-7 reveal an atypical oligomeric conformation compared to phospholipases A₂-like toxins. *Biochimie* **142**, 11–21 (2017).
- Watanabe, L., Soares, A. M., Ward, R. J., Fontes, M. R. M. & Arni, R. K. Structural insights for fatty acid binding in a Lys49-phospholipase A₂: Crystal structure of myotoxin II from *Bothrops moojeni* complexed with stearic acid. *Biochimie* **87**, 161–167 (2005).
- Toyama, D. *et al.* Umbelliferone induces changes in the structure and pharmacological activities of Bn IV, a phospholipase A₂ isoform isolated from *Bothrops neuwiedi*. *Toxicon* **57**, 851–860 (2011).
- Salvador, G. H. M. *et al.* Structural and functional studies with myotoxin II from *Bothrops moojeni* reveal remarkable similarities and differences compared to other catalytically inactive phospholipases A₂-like. *Toxicon* **72**, 52–63 (2013).
- Magro, A. J., Soares, A. M., Giglio, J. R. & Fontes, M. R. M. Crystal structures of BnSP-7 and BnSP-6, two Lys49-phospholipases A₂: Quaternary structure and inhibition mechanism insights. *Biochem. Biophys. Res. Commun.* **311**, 713–720 (2003).
- Murakami, M. T. *et al.* Interfacial surface charge and free accessibility to the PLA₂-active site-like region are essential requirements for the activity of Lys49 PLA₂ homologues. *Toxicon* **49**, 378–387 (2007).
- dos Santos, J. I., Soares, A. M. & Fontes, M. R. M. Comparative structural studies on Lys49-phospholipases A₂ from *Bothrops* genus reveal their myotoxic site. *J. Struct. Biol.* **167**, 106–116 (2009).
- Salvador, G. H. M. *et al.* Structural and Phylogenetic Studies with MjTX-I Reveal a Multi-Oligomeric Toxin - a Novel Feature in Lys49-PLA₂s Protein Class. *PLoS One* **8**, e60610 (2013).
- Murakami, T. *et al.* Island specific expression of a novel [Lys⁴⁹]phospholipase A₂ (BPIII) in *Protobothrops flavoviridis* venom in Amami-Oshima, Japan. *Toxicon* **54**, 399–407 (2009).
- Ohno, M., Chijiwa, T., Oda-Ueda, N., Ogawa, T. & Hattori, S. Molecular evolution of myotoxic phospholipases A₂ from snake venom. *Toxicon* **42**, 841–854 (2003).
- Kabsch, W. Xds. *Acta Crystallogr. D. Biol. Crystallogr.* **66**, 125–132 (2010).
- McCoy, A. J. Solving structures of protein complexes by molecular replacement with Phaser. *Acta Crystallogr. D. Biol. Crystallogr.* **63**, 32–41 (2007).

28. Afonine, P. V. *et al.* Towards automated crystallographic structure refinement with phenix.refine. *Acta Crystallogr. D. Biol. Crystallogr.* **68**, 352–367 (2012).
29. Emsley, P. & Cowtan, K. Coot: model-building tools for molecular graphics. *Acta Crystallogr. D, Biol. Crystallogr.* **60**, 2126–2132 (2004).
30. Chen, V. B. *et al.* MolProbity: all-atom structure validation for macromolecular crystallography. *Acta Crystallogr. D. Biol. Crystallogr.* **66**, 12–21 (2010).
31. Schrödinger, L. L. C. The JyMOL Molecular Graphics Development Component, Version 1.0 (2010).
32. Ishii, K. *et al.* Disassembly of the self-assembled, double-ring structure of proteasome $\alpha 7$ homo-tetradecamer by $\alpha 6$. *Sci. Rep.* **5**, 18167 (2015).
33. Schuck, P. Size-distribution analysis of macromolecules by sedimentation velocity ultracentrifugation and Lamm equation modeling. *Biophys. J.* **78**, 1606–1619 (2000).
34. Brown, P. H., Balbo, A., Zhao, H., Ebel, C. & Schuck, P. Density contrast sedimentation velocity for the determination of protein partial-specific volumes. *PLoS One* **6**, 18167 (2011).
35. Nango, E. *et al.* Taste substance binding elicits conformational change of taste receptor T1r heterodimer extracellular domains. *Sci. Rep.* **6**, 18167 (2016).
36. Schuck, P. On the analysis of protein self-association by sedimentation velocity analytical ultracentrifugation. *Anal. Biochem.* **320**, 104–124 (2003).
37. Tanford, C., Nozaki, Y., Reynolds, J. A. & Makino, S. Molecular Characterization of Proteins in Detergent Solutions. *Biochemistry* **13**, 2369–2376 (1974).
38. Miyabe, K., Takahashi, R. & Shimazaki, Y. Kinetic Study of Interaction between Solute Molecule and Surfactant Micelle. *Anal Sci* **31**, 1019–1025 (2015).
39. Liu, Q. *et al.* The crystal structure of a novel, inactive, lysine 49 PLA₂ from *Agkistrodon acutus* venom: An ultrahigh resolution, ab initio structure determination. *J. Biol. Chem.* **278**, 41400–41408 (2003).
40. Arni, R. K. *et al.* Crystal structure of myotoxin II, a monomeric Lys49-phospholipase A₂ homologue isolated from the venom of *Cerrophidion (Bothrops) godmani*. *Arch. Biochem. Biophys.* **366**, 177–182 (1999).
41. Da Silva Giotto, M. T. *et al.* Crystallographic and spectroscopic characterization of a molecular hinge: Conformational changes in Bothropstoxin I, a dimeric Lys49-phospholipase A₂ homologue. *Proteins Struct. Funct. Genet.* **30**, 442–454 (1998).
42. Ullah, A., Souza, T. A. C. B., Betzel, C., Murakami, M. T. & Arni, R. K. Crystallographic portrayal of different conformational states of a Lys49 phospholipase A₂ homologue: Insights into structural determinants for myotoxicity and dimeric configuration. *Int. J. Biol. Macromol.* **51**, 209–214 (2012).
43. Kilby, P. M., Primrose, W. U. & Roberts, G. C. Changes in the structure of bovine phospholipase A₂ upon micelle binding. *Biochem. J.* **305**, 935–944 (1995).
44. Duplâtre, G., Ferreira Marques, M. F. & da Graça, M. M. Size of Sodium Dodecyl Sulfate Micelles in Aqueous Solutions as Studied by Positron Annihilation Lifetime Spectroscopy. *J. Phys. Chem.* **100**, 16608–16612 (1996).

Acknowledgements

The X-ray diffraction experiments were performed at the Photon Factory (proposals 16G092, 18G060, and 17G595) and SPring-8 (proposals 2015B6524, 2016A2565 and 2016B2565). This work was supported in part by the following sources: the Grants-in-Aid for Scientific Research from the Ministry of Education, Culture, Sports, Science and Technology, Japan (to T.Matsui and Y.T.), the PRESTO (to Y.T.), the Joint Research by Exploratory Research Center on Life and Living Systems (ExCELLS) (to SU and KK), and the Platform Project for Supporting Drug Discovery and Life Science Research [Basis for Supporting Innovative Drug Discovery and Life Science Research (BINDS)] from the Japan Agency for Medical Research and Development (AMED) under Grant Number JP18am0101095 (to T.Matsui). This research was also supported by a JSPS Grants-in-Aid for Scientific Research on Innovative Areas entitled “Dynamical Ordering of Biomolecular Systems for Creation of Integrated Functions” (25102008, 16H00770, and 16H00748), NEDO, and JICE.

Author Contributions

T. Matsui, T.O. and Y.T. designed the experiments. T. Matsui, S.K., K.I., T. Maruno, N.G. and A.S. performed the experiments. T. Matsui, S.K., K.I., T. Maruno, N.G., S.U. and Y.T. analyzed the data. T. Matsui, S.K., S.U., K.K., N.O.-U. and Y.T. wrote the paper. All authors reviewed the results and approved the final version of the manuscript.

Additional Information

Supplementary information accompanies this paper at <https://doi.org/10.1038/s41598-019-38861-8>.

Competing Interests: The authors declare no competing interests.

Publisher's note: Springer Nature remains neutral with regard to jurisdictional claims in published maps and institutional affiliations.



Open Access This article is licensed under a Creative Commons Attribution 4.0 International License, which permits use, sharing, adaptation, distribution and reproduction in any medium or format, as long as you give appropriate credit to the original author(s) and the source, provide a link to the Creative Commons license, and indicate if changes were made. The images or other third party material in this article are included in the article's Creative Commons license, unless indicated otherwise in a credit line to the material. If material is not included in the article's Creative Commons license and your intended use is not permitted by statutory regulation or exceeds the permitted use, you will need to obtain permission directly from the copyright holder. To view a copy of this license, visit <http://creativecommons.org/licenses/by/4.0/>.

© The Author(s) 2019